System Evaluation

The practicability of the proposed manual system rests upon certain premises. First, the navigator must have the ability to collect a sufficient amount of data during a prescribed interval and to perform the necessary computations within a specified interval without error. Also, the astronauts must be capable of orienting the vehicle relative to a star reference, holding this orientation for the interval of thrust, and terminating thrust within a certain time error. Finally, the approximation of the system must not produce intolerable errors.

A navigator's ability to measure 12 or more time varying angles with an accuracy of 10 sec of arc in a short time interval (about 30 min for a lunar mission) and to orient the vehicle using a star reference can be rested only by simulation. Such experiments were not undertaken.

An estimate of the required time for computation, however, was made. A series of experiments was performed using a simulated lunar mission to measure the interval of time required for equation computation. The navigator's program for two velocity corrections was evaluated a number of times. The average time interval of calculation for one velocity correction was 24 min, which includes the plotting and computation but not the angle measurement interval. The computations were performed with an ordinary slide rule and the results were sufficiently accurate.

A first-order analytical error analysis of the manual guidance and navigation system was undertaken using a typical lunar mission. The components of independent error source vector $\mathbf{E}$ were chosen to be in initial injection position $\mathbf{X}_0$, the measured angles $\boldsymbol{\alpha}$, the time axis of the interpolation graph t, thrust termination timing τ, and thrust orientation $\rho = (\gamma,\delta)$. The errors in these variables were assumed to be Gaussian and uncorrelated with means of zero. The covariance matrix cov($\mathbf{E}$) of these variables is diagonal and the diagonal elements were taken as

$$[\sigma\mathbf{X}_0^2,(\sigma_\alpha^2 + \dot{\alpha}^2\sigma_t^2)/N, A^2\sigma_\tau^2 + 2|\mathbf{V}_g|^2\sigma_\rho^2]$$

where N is an empirical number representing the improvement of the accuracy of the interpolated angles due to the graphical smoothing process. The diagonal elements represent three classes of error: initial position, measurement data reduction, and execution of velocity correction. The dependent variables to be examined for error were the position and velocity $\mathbf{F} = (x,y,z,\dot{x},\dot{y},\dot{z})$ at various times along the trajectory. The covariance matrix cov($\mathbf{F}$) of the final position and velocity was approximated as

$$\text{cov}(\mathbf{F}) \approx (\partial\mathbf{F}/\partial\mathbf{E})^T\text{cov}(\mathbf{E})(\partial\mathbf{F}/\partial\mathbf{E})$$

where the symbol T denotes the transpose and where $(\partial\mathbf{F}/\partial\mathbf{E})$ represents a 6×9 matrix whose elements are the derivatives of the final variables with respect to the independent error source variables. Figure 2 gives typical numerical results of finding the square roots of eigenvalues of cov($\mathbf{F}$) at critical times along the lunar trajectory. The numbers are pessimistic since a conservative upper bound on $\mathbf{V}_g$ was used, no improvement was assumed in using redundant data ($N = 1$), and no attempt was made to minimize the value of the guidance constants by proper choice of stars or times of the measurement taking and course correction.

The equation errors of the manual system were examined for a number of typical lunar trajectories. It was found that if the maximum deviation from the nominal is less than 400 naut miles, the resulting errors due to equation approximation in the neighborhood of the moon were less than 1 naut mile in position and 1 fps in velocity. If, however, large deviations from the nominal are expected, the guidance constants, the elements of G_1 and G_2, can be made as linear or higher order functions of the deviations of $\Delta\alpha$ from nominal to circumvent equation error. This will increase the computation load upon the navigator but not intolerably.

MAXIMUM ERRORS IN EARTH GEOCENTRIC RECTANGULAR COORDINATES

	t	σ_x	σ_y	σ_z	$\sigma_{\dot{x}}$	$\sigma_{\dot{y}}$	$\sigma_{\dot{z}}$
	hr	n.mi.	n.mi.	n.mi.	fps	fps	fps
FIRST CORRECTION	9	3.4	43.1	29.0	11.3	14.7	1.9
SECOND CORRECTION	63	1.6	12.1	7.6	5.1	5.4	3.7
MOON VICINITY	77	54.5	36.8	24.1	14.0	2.4	1.3

PARAMETER ASSUMPTIONS

- SMOOTHING IMPROVEMENT FACTOR N=1
- VELOCITY CORRECTION MAGNITUDE $|V_g|$ = 200 fps.

INPUT ERROR ASSUMPTIONS

- INITIAL POSITION $(\sigma_x, \sigma_y, \sigma_z)$ = (1,1,1) n. mi.
- ANGULAR MEASUREMENT AND PLOT $(\sigma_{\alpha 1}, \sigma_{\alpha 2}, \sigma_{\alpha 3})$ = (10,10,10) sec
- TIME MEASUREMENT AND PLOT σ_t = 10 sec.
- THRUST TIMING σ_τ = .1 sec
- THRUST ORIENTATION σ_ρ = 1 deg

Fig. 2 System error analysis.

Conclusion

A completely manual extraterrestrial guidance and navigation system is feasible from a computational point of view. The ability of an astronaut to obtain sufficient measurement data during a short time interval is yet to be demonstrated. The technique of manually orienting a vehicle to a preferred direction and to perform a velocity correction has been demonstrated by the Mercury flights. The somewhat degraded accuracy of a manual system over an automatic system is to be expected. These considerations indicate that the design and study of a manned system for emergency backup or monitor should be pursued with the utmost vigor.

Body Force Effects on Transient Melting and Vaporizing Ablation

SHIH-YUAN CHEN*
The Boeing Company, Seattle, Wash.

A space vehicle or a ballistic missile re-entering the earth's atmosphere experiences a large aerodynamic drag force in the dense atmospheric region. This drag force, in turn, produces a decelerated motion to slow down the vehicle or missile along its trajectory. In general, ground static transient tests of melting ablation will not be able to simulate this type of decelerated motion. An analysis is made to determine body force effects due to acceleration or deceleration in the stagnation region for melting glassy materials. Within the ranges of values investigated, the results indicate that the transient static tests predict an ablation rate that can be either as much as 23% higher than

Received by ARS December 10, 1962; revision received June 28, 1963. The author wishes to express his gratitude to B. F. Beckelman, Chief of Flight Technology, Aero-Space Division, The Boeing Company, for his interest, encouragement, and permission to publish this material; to H. Kennet, O. A. Huseby, and M. B. Donovan, all of the Advanced Research Section, for their valuable suggestions and comments; and to S. L. Adams for her typing.

* Chief, Advanced Research Section, Flight Technology Department, Aero-Space Division. Associate Fellow Member AIAA.

that encountered by a decelerating vehicle or as much as 17% lower than that experienced by an accelerating vehicle.

Nomenclature

a = constant parameter describing the unsteadiness of the inviscid gas flow
c_p = specific heat at constant pressure
c_v = specific heat at constant volume
C = a constant parameter describing velocity at the edge of the gas boundary layer
f = dimensionless stream function
J = mechanical equivalent of heat
k = thermal conductivity
$\dot{m}$ = mass transfer rate
n = exponent in viscosity
p = pressure
R = gas constant
R_B = body radius of curvature
r_0 = body cross-sectional radius
T = temperature
u = velocity component in the x direction
v = velocity component in the y direction
U_∞ = freestream velocity
X = body force in x direction
x = coordinate parallel to body surface
Y = body force in y direction
y = coordinate normal to body surface
α = thermal diffusivity
θ = dimensionless temperature
μ = coefficient of viscosity
ρ = density
σ = Prandtl number
τ = time, also shear stress

Subscripts

e = edge of gas boundary layer
i = gas-liquid interface

Superscripts

$*$ = any arbitrary reference temperature
$'$ = differentiation with respect to η
ϵ = geometrical constant: = 0 for planar body; = 1 for body of revolution

Introduction

PERFORMANCE evaluation of ablating materials in arc-wind tunnels or plasma-jet facilities can simulate the transient thermal environment. However, the decelerated motion experienced by a vehicle during re-entry cannot be simulated in these facilities at the present time.

Recently, Chen and Allen[1] neglected the inertia terms and used a similarity analysis to obtain solutions without body force effects. The results show that transient effects cannot be ignored. In other words, steady-state ground static tests predict a different melting ablation rate than that of transient ground static tests. The purpose of this paper is to extend the investigation[1] to determine quantitatively the effects of body force and density ratio on melting and vaporizing ablation on bluntnosed bodies.

General Governing Equations

The general conservative equations for the laminar incompressible liquid layer are

Continuity

$$(\partial/\partial x)(r_0^\epsilon u) + (\partial/\partial y)(r_0^\epsilon v) = 0 \qquad (1)$$

where $\epsilon = 0$ for a planar body, and $\epsilon = 1$ for a body of revolution.

Momentum

$$\rho\left(\frac{\partial u}{\partial \tau} + u\frac{\partial u}{\partial x} + v\frac{\partial u}{\partial y}\right) = \frac{\partial \rho}{\partial x} + X + \frac{\partial}{\partial y}\left(\mu\frac{\partial u}{\partial y}\right) \qquad (2)$$

$$0 = -\frac{\partial p}{\partial y} + Y \qquad (3)$$

Energy

$$\rho c v\left(\frac{\partial u}{\partial \tau} + u\frac{\partial T}{\partial x} + v\frac{\partial T}{\partial y}\right) = \frac{\partial}{\partial y}\left(k\frac{\partial T}{\partial y}\right) + \mu\left(\frac{\partial u}{\partial y}\right)^2 \qquad (4)$$

The nomenclature, assumptions, definitions, and transformations are the same as in Ref. 1.

Equation (3) can be rewritten approximately as

$$Y = (\partial p/\partial x) \cong \rho(\partial U_\infty/\partial \tau)$$

or

$$\Delta p \cong \rho(\partial U_\infty/\partial \tau)\Delta y$$

The value of Δp is very small because the thickness of Δy is generally very thin. Therefore,

$$(\partial p/\partial x) \cong (dp/dx) \cong (dp_e/dx) \qquad (5)$$

is assumed for practical purposes, or

$$-\frac{\partial p}{\partial x} = \rho_e\left(\frac{\partial u_e}{\partial \tau} + u_e\frac{\partial u_e}{\partial x}\right) - X_e \qquad (6)$$

where $X = \rho\,(x/R_B)(\partial u/\partial \tau)$ is the body force at the edge of the gas boundary layer. The velocity at the edge of the gas is assumed to vary in a hyperbolic manner with time,[1,3] namely,

$$u_e = Cx/(1 - Ca\tau) \qquad (7)$$

where C is a function of re-entry velocity and a is a function of ballistic coefficient.

Substituting Eqs. (6) and (7) into Eq. (2), one obtains

$$\rho\left(\frac{\partial u}{\partial \tau} + u\frac{\partial u}{\partial x} + v\frac{\partial u}{\partial y}\right) = \rho_e x\left(\frac{u_e}{x}\right)^2(a+1) + \frac{\partial}{\partial y}\left(\mu\frac{\partial u}{\partial y}\right) + \rho\frac{x}{R_B}\frac{\partial U_\infty}{\partial \tau} \qquad (8)$$

Introducing the Levy and Mangler transforms,[1,2] Eqs. (8) and (4) become

$$2\left(\frac{\mu}{\mu^*}f''\right)' + 2ff'' - (f')^2 + \frac{\rho_e}{\rho} = a\left[f''\frac{\eta}{2} + f' - \frac{\rho_e}{\rho} - \left(\frac{Jc_p}{R}\right)^{1/2}\right] \qquad (9)$$

$$2\theta'' + \sigma^*\theta'\left(2f - \frac{a\eta}{2}\right) - 2a\sigma^*\theta = 0 \qquad (10)$$

where

$f(\eta)$ = a dimensionless stream function
θ = a dimensionless temperature quantity
σ^* = $\rho\alpha/\varphi^*$
η = $\left(\frac{2\rho}{\mu^*}\frac{C}{1 - Ca\tau}\right)^{1/2} y$
μ $\propto T^{-n}$
$(Jcp/R)^{1/2} \cong 2.45$ for $\gamma_{av}^* \cong 1.2$

In practical application, $(\rho_e/\rho) \ll 2.45$ and can be neglected on the right-hand side of Eq. (9), or

$$2\left(\frac{\mu}{\mu^*}f''\right)' + 2ff'' - (f')^2 + \frac{\rho_e}{\rho} = a\left(f''\frac{\eta}{2} + f' - 2.45\right) \qquad (11)$$

The associated boundary conditions are

$$\frac{\partial u(0)}{\partial y} = -\frac{\tau_i}{\mu_i} \qquad v(0) = -\frac{\dot{m}_i}{\rho} \qquad T(0) = T_i$$

$$\lim_{\eta\to\infty} u = 0 \qquad \lim_{\eta\to\infty}\frac{\partial T}{\partial y} = 0$$

which are the same as given by Chen and Allen.[1]

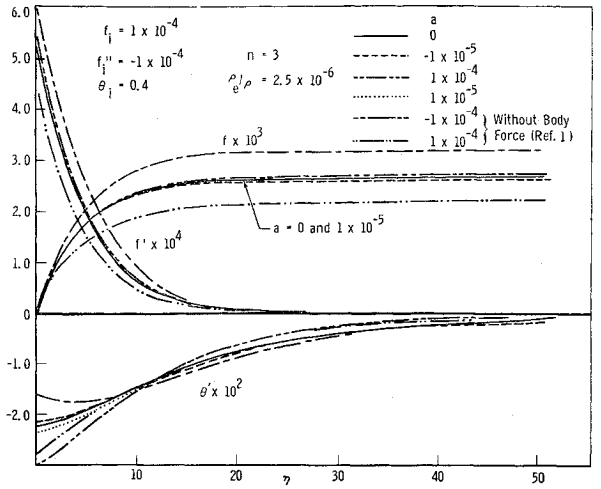

Fig. 1 Transient and body force effects on velocity distribution and heat transfer.

The transformed boundary conditions become

$$f''(0) = f_i'' \qquad f(0) = f_i \qquad \theta(0)\ \theta_i$$

$$\lim_{\eta \to \infty} f' = 0 \qquad \lim_{\eta \to \infty} \theta' = 0$$

where f_i'', f_i, and θ are parameters. The method of solution is the same as that given in Ref. 1.

Discussion and Conclusions

Figure 1 shows the effects of a on ablation rate, velocity, and heat transfer at the gas-liquid interface. One immediately notices that, for the given boundary conditions at the gas-liquid interface, the effects of body force are to reduce both transient effects on nondimensional albation velocity $f(\infty)$ and nondimensional velocity component f'. It is found that nondimensional ablation velocity $f(\infty)$ is 17% greater than the static transient value (no body force) in the nonflowing solid interior for accelerated motion $a = 1 \times 10^{-4}$ and is approximately equal to steady state value ($a = 0$). On the other hand, for decelerated motion, there is a corresponding 23% decrease in $f(\infty)$ for $a = 1 \times 10^{-4}$. This indicates that a static transient test predicts a higher ablation velocity than actually experienced by a decelerated vehicle. For an accelerated vehicle, the static transient test predicts a lower ablation velocity.

In Ref. 1, it is found that some of the nondimensional heat-transfer rate profiles display a maximum value for finite η. It should be pointed out that η is a function of τ and y. One can also obtain the value of η, where maximum or minimum

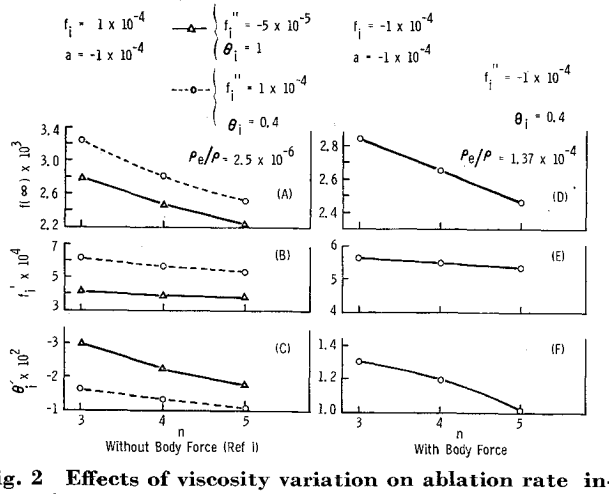

Fig. 2 Effects of viscosity variation on ablation rate interface velocity, and interface heat transfer rate.

heat transfer rate occurs from energy Eq. (10) by setting $\theta'' = 0$ and obtaining $\eta = (4f/a) - (4\theta/\theta')$. Figure 1 also shows that the heat transfer rate at the gas-liquid interface appears to have no correlation with body force effects.

Figure 2 shows the effects of viscosity variation with and without body force. In general, an increase in n causes a decrease in the nondimensional ablation velocity, the nondimensional interface velocity, and the nondimensional interface heat transfer rate. However, the effects are considerably smaller for cases with body force. It is seen that the ablation rate is reduced by 22% without body force for $\rho_e/\rho = 2.5 \times 10^{-6}$ and by only 12.8% with body force for $\rho_e/\rho = 1.37 \times 10^{-4}$, n is increased from 3 to 5. The effects of n on the nondimensional interface heat transfer rate θ_i' is also smaller with body force or reduces to 23% as n increases from 3 to 5 (35% for no body force case). In general, these reductions for increased values of n are believed to be due to the increase in the viscosity coefficient, which, in turn, enables the molten flowing liquid to stay longer locally (smaller velocity) and at a higher internal temperature.

Figure 3 shows the effects of density ratio. In general, for a constant ρ an increase in the density of the ablation material results in a decrease in the ablation velocity. Another way to look at this is to assume ρ constant. Then a decrease in ρ_e/ρ indicates a higher altitude. Thus, for the

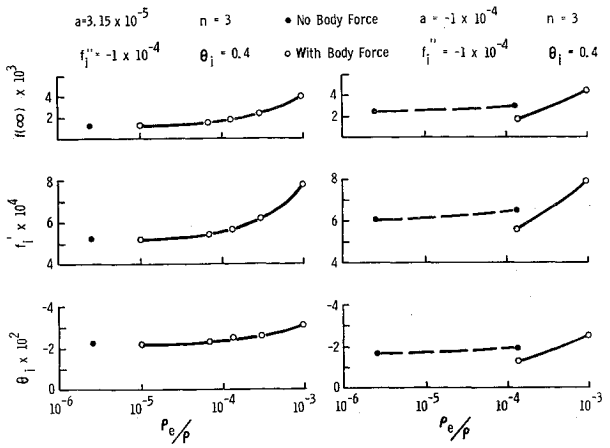

Fig. 3 Effects of density variation on ablation rate, velocity, and heat transfer rate at gas-liquid interface.

same ablation material, the ablation rates increase with a decrease in altitude.

The thickness of the molten-flowing region, which is about one-third that of the heated region is, generally, not affected by the body force. This is also true for the case without body force. At $\eta = 20$, the nondimensional heat transfer rate θ' is approximately 25 to 50% of that at the gas-liquid interface.[1] In other words, the liquid layer absorbed is about 50 to 75% of the energy transmitted at the gas-liquid interface.

From this study, it appears that the static transient test cannot supply accurate information on ablation velocity for a high performance re-entry vehicle. For the conditions investigated, this can cause an error of as much as 23%. The inclusion of body force effects tends to reduce the transient effects on ablation velocity to the steady state value.

References

[1] Chen, S. Y. and Allen, S. J., "Similarity analysis for transient melting and vaporizing ablation on blunt-nosed bodies," ARS J. **32**, 1536–1543 (1962).

[2] Sutton, G. W., "The hydrodynamics and heat conduction of a melting surface," J. Aeronaut. Sci. **25**, 29–32 (1958).

[3] Yang, Kwang-Tzu, "Unsteady laminar boundary layers in an incompressible stagnation flow," J. Appl. Mech. **25**, 421–427 (December 1958).